

Calculation of the hadronic vacuum polarization disconnected contribution to the muon anomalous magnetic moment

T. Blum,¹ P.A. Boyle,² T. Izubuchi,^{3,4} L. Jin,⁵ A. Jüttner,⁶ C. Lehner,^{3,*}
K. Maltman,^{7,8} M. Marinkovic,⁹ A. Portelli,^{2,6} and M. Spraggs⁶

(RBC and UKQCD Collaborations)

¹*Physics Department, University of Connecticut, Storrs, CT 06269-3046, USA*

²*SUPA, School of Physics, The University of Edinburgh, Edinburgh EH9 3JZ, UK*

³*Physics Department, Brookhaven National Laboratory, Upton, NY 11973, USA*

⁴*RIKEN-BNL Research Center, Brookhaven National Laboratory, Upton, NY 11973, USA*

⁵*Physics Department, Columbia University, New York, NY 10027, USA*

⁶*School of Physics and Astronomy, University of Southampton, Southampton SO17 1BJ, UK*

⁷*Mathematics & Statistics, York University, Toronto, ON, M3J 1P3, Canada*

⁸*CSSM, University of Adelaide, Adelaide 5005 SA, Australia*

⁹*CERN, Physics Department, 1211 Geneva 23, Switzerland*

(Dated: December 30, 2015)

We report the first lattice QCD calculation of the hadronic vacuum polarization disconnected contribution to the muon anomalous magnetic moment at physical pion mass. The calculation uses a refined noise-reduction technique which enabled the control of statistical uncertainties at the desired level with modest computational effort. Measurements were performed on the $48^3 \times 96$ physical-pion-mass lattice generated by the RBC and UKQCD collaborations. We find $a_\mu^{\text{HVP (LO) DISC}} = -9.6(3.3)(2.3) \times 10^{-10}$, where the first error is statistical and the second systematic.

PACS numbers: 12.38.Gc

INTRODUCTION

The anomalous magnetic moment of leptons provides a powerful tool to test relativistic quantum-mechanical effects at tremendous precision. Consider the magnetic dipole moment of a fermion

$$\vec{\mu} = g \left(\frac{e}{2m} \right) \vec{s}, \quad (1)$$

where \vec{s} is the particle's spin, e is its charge, and m is its mass. While Dirac's relativistic quantum-mechanical treatment of a fermion coupled minimally to a classical photon background predicts a Landé factor of $g = 2$, additional electromagnetic quantum effects allow the anomalous magnetic moment $a = (g - 2)/2$ to assume a non-zero value. These anomalous moments are measured very precisely. For the electron, e.g., $a_e = 0.00115965218073(28)$ [1] yielding the currently most precise determination of the fine structure constant $\alpha = 1/137.035999157(33)$ based on a 5-loop quantum electrodynamics (QED) computation [2].

The muon anomalous magnetic moment promises high sensitivity to new physics (NP) beyond the standard model (SM) of particle physics. In general, new physics contributions to a_ℓ are expected to scale as $a_\ell - a_\ell^{\text{SM}} \propto (m_\ell^2/\Lambda_{\text{NP}}^2)$ for lepton $\ell = e, \mu, \tau$ and new physics scale Λ_{NP} . With a_τ being currently experimentally inaccessible, a_μ is the optimum channel to uncover new physics.

Interestingly, there is an $3.1\text{--}3.5\sigma$ tension between cur-

rent experimental and theoretical determinations of a_μ ,

$$a_\mu^{\text{EXP}} - a_\mu^{\text{SM}} = (27.6 \pm 8.0) \times 10^{-10} [3], \\ (25.0 \pm 8.0) \times 10^{-10} [4], \quad (2)$$

where the experimental measurement is dominated by the BNL experiment E821 [5]. The theoretical prediction [6] is broken down in individual contributions in Tab. I.

The theory error is dominated by the hadronic vacuum polarization (HVP) and hadronic light-by-light (HLbL) contributions. A careful first-principles determination of these hadronic contributions is very much desired to resolve or more firmly establish the tension with the current SM prediction. Furthermore, the future a_μ experiments at Fermilab (E989) [7] and J-PARC (E34) [8] intend to decrease the experimental error by a factor of four. Therefore a similar reduction of the theory error is essential in order to make full use of the experimental efforts.

The current SM prediction for the HLbL [11] is based on a model of quantum chromodynamics (QCD), however, important progress towards a first-principles computation has been made recently [12–14]. The uncertainty of the HVP contribution may be reduced to $\delta a_\mu = 2.6 \times 10^{-10}$ using improved experimental e^+e^- scattering data [9]. An ab-initio theory prediction based on QCD, however, can provide an important alternative determination that is systematically improvable to higher precision.

One of the main challenges in the first-principles computation of the HVP contribution with percent or sub-percent uncertainties is the control of statistical noise

Contribution	Value $\times 10^{10}$	Uncertainty $\times 10^{10}$
QED	11 658 471.895	0.008
Electroweak Corrections	15.4	0.1
HVP (LO) [3]	692.3	4.2
HVP (LO) [4]	694.9	4.3
HVP (NLO)	-9.84	0.06
HVP (NNLO)	1.24	0.01
HLbL	10.5	2.6
Total SM prediction [3]	11 659 181.5	4.9
Total SM prediction [4]	11 659 184.1	5.0
BNL E821 result	11 659 209.1	6.3
Fermilab E989 target		≈ 1.6

TABLE I. Current standard model prediction of a_μ including uncertainties contrasted with the experimental target precision of the upcoming Fermilab E989 experiment [6, 9, 10]. The individual contributions are defined in Ref. [6].

for the quark-disconnected contribution (see Fig. 1) at physical pion mass. Significant progress has been made recently in the computation of an upper bound [15–17], an estimate using lattice QCD data at heavy pion mass [18], and towards a first-principles computation at physical pion mass [19]. Here we present the first result for $a_\mu^{\text{HVP (LO) DISC}}$ at physical pion mass. We report the result for the combined up, down, and strange quark contributions.

COMPUTATIONAL METHOD

In the following we describe the refined noise-reduction technique that allowed for the control of the statistical noise with modest computational effort.

We follow the basic steps of Ref. [20] and treat the muon and photon parts of the diagrams in Fig. 1 analytically, writing

$$a_\mu = 4\alpha^2 \int_0^\infty d(q^2) f(q^2) [\Pi(q^2) - \Pi(q^2 = 0)], \quad (3)$$

where $f(q^2)$ is a known analytic function [20] and $\Pi(q^2)$ is defined in the continuum through the two-point function

$$\sum_x e^{iqx} \langle J_\mu(x) J_\nu(0) \rangle = (\delta_{\mu\nu} q^2 - q_\mu q_\nu) \Pi(q^2) \quad (4)$$

with sum over space-time coordinate x and $J_\mu(x) = i \sum_f Q_f \bar{\Psi}_f(x) \gamma_\mu \Psi_f(x)$. The sum is over quark flavors f with QED charge Q_f ($Q_u = 2/3$, $Q_{d/s} = -1/3$). We compute $\Pi(q^2)$ using the kernel function of Refs. [21, 22]

$$\Pi(q^2) - \Pi(q^2 = 0) = \sum_t \left(\frac{\cos(qt) - 1}{q^2} + \frac{1}{2} t^2 \right) C_{\text{all}}(t) \quad (5)$$

with

$$C_{\text{all}}(t) = \frac{1}{3} \sum_{\vec{x}} \sum_{j=0,1,2} \langle J_j(\vec{x}, t) J_j(0) \rangle \quad (6)$$

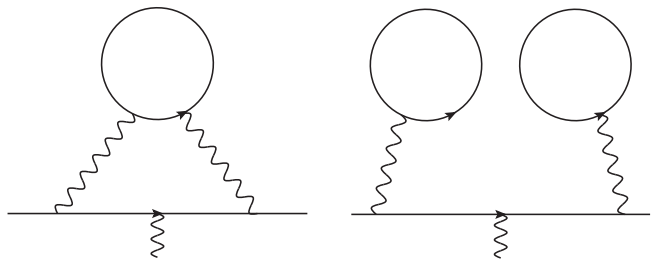


FIG. 1. HVP contributions to a_μ with external photon attached to the muon line. As common for non-perturbative lattice QCD computations, one does not explicitly draw gluons but understands each diagram to stand for all orders in QCD.

which sufficiently suppresses the short-distance contributions such that we are able to use two less computationally costly, non-conserved, local lattice vector currents [23]. For convenience, we have split the space-time sum over x in a spatial sum over \vec{x} and a sum over the time coordinate t . We sum over spatial Lorentz indices 0, 1, 2.

The Wick contraction in Eq. (6) yields both connected and disconnected diagrams of Fig. 1. In the following C stands for the combined up-, down-, and strange-quark disconnected contribution of C_{all} , while C_s stands for the strange-quark connected contribution of C_{all} . The reason for defining C_s will become apparent below. The light up and down flavors are treated as mass degenerate such that

$$C(t) = \frac{1}{3V} \sum_{j=0,1,2} \sum_{t'} \langle \mathcal{V}_j(t+t') \mathcal{V}_j(t') \rangle_{\text{SU}(3)} \quad (7)$$

where V stands for the four-dimensional lattice volume, $\mathcal{V}_\mu = (1/3)(\mathcal{V}_\mu^{u/d} - \mathcal{V}_\mu^s)$, the average is over all SU(3) gauge configurations, and

$$\mathcal{V}_\mu^f(t) = \sum_{\vec{x}} \text{Im Tr} [D_{\vec{x},t;\vec{x},t}^{-1}(m_f) \gamma_\mu] \quad (8)$$

with Dirac operator $D(m_f)$ evaluated at quark mass m_f .

Controlling statistical fluctuations is the largest challenge in the computation of the disconnected contribution. In order to successfully measure the disconnected contribution, two conditions need to be satisfied: (i) large fluctuations of the up/down and strange contributions that enter with opposite sign need to cancel [15] and (ii) the measurement needs to average over the entire spacetime volume without introducing additional noise. Here we use the following method to satisfy both (i) and (ii) simultaneously. First, the full quark propagator is separated in high and low-mode contributions, where the former are estimated stochastically and the latter are averaged explicitly [24], i.e., we separate $D^{-1} = \sum_n v^n (w^n)^\dagger + D_{\text{high}}^{-1}$, where the vectors v^n and w^n are reconstructed from the even-odd preconditioned

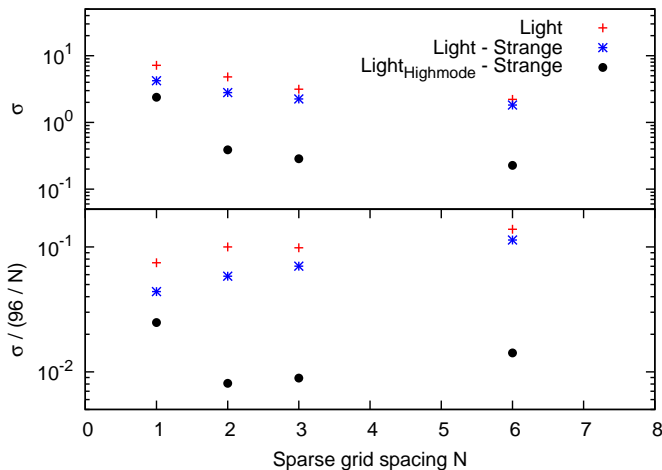


FIG. 2. Noise of single vector operator loop as a function of sparse grid spacing N . The figure at the bottom normalizes the noise by taking into account the additional volume averaging for smaller values of N .

low-modes n of the Dirac propagator D^{-1} . It is now crucial to include all modes with eigenvalues up to the strange quark mass in the set of low modes for the up and down quark propagators to satisfy (i). Since the signal is the difference of light and strange contributions, we may then expect the high-mode contribution to be significantly suppressed and the low-mode contribution to contain the dominant part of the signal. This is indeed the case in our computation and yields a substantial statistical benefit since we evaluate the low modes exactly without the introduction of noise and average explicitly over the entire volume.

In order to satisfy (ii), we must control the stochastic noise of the high-mode contributions originating from unwanted long-distance contributions of the random Z_2 sources of Ref. [24]. We achieve this by using what we refer to as sparsened Z_2 noise sources which have support only for points x_μ with $(x_\mu - x_\mu^{(0)}) \bmod N = 0$ thereby defining a sparse grid with spacing N , similar to Ref. [25]. While a straightforward dilution strategy [24] would require us to sum over all possible offsets of the sparse noise grid, $x_\mu^{(0)}$, we choose the offset stochastically for each individual source which allows us to project to all momenta. It also allows us to avoid the largest contribution of such random sources to the noise which comes from random sources at nearby points.

The parameter choice of N is crucial to satisfy (ii) with minimal cost. Figure 2 shows the square root of the variance σ^2 of \mathcal{V} on a single lattice configuration over time coordinate t and Lorentz index μ . Since we can use all possible $O(M^2)$ combinations of M high-mode sources and time-coordinates in Eq. (7), we may expect a noise suppression of $O(1/M)$ as long as individual contributions are sufficiently statistically independent. A similar

idea of $O(1/M)$ noise reduction was recently successfully used in Ref. [12]. We find this to hold to a large degree, and therefore also show the appropriately rescaled σ in the lower panel of Fig. 2. The figure illustrates the powerful cancellation of noise between the light and strange quark contributions and the success of the sparsening strategy. We find an optimum value of $N = 3$ for the case at hand, which is used for the subsequent numerical discussion.

We use 45 stochastic high-modes per configuration and measure on 21 Moebius domain wall [26] configurations of the $48^3 \times 96$ ensemble at physical pion mass and lattice cutoff $a^{-1} = 1.73$ GeV generated by the RBC and UKQCD collaborations [27]. For this number of high modes we find the QCD gauge noise to dominate the uncertainty for $a_\mu^{\text{HVP (LO) DISC}}$. The AMA strategy [28, 29] was employed to reduce the cost of computing multiple sources on the same configuration. The computation presented in this manuscript uses 2000 zMobius [30] eigenvectors generated as part of an on-going HLbL lattice computation [12]. We treat the shorter directions with 48 points as the time direction and average over the three symmetric combinations to further reduce stochastic noise.

ANALYSIS AND RESULTS

Combining Eqs. (3) and (5) and using $C(t) = C(-t)$,

$$a_\mu^{\text{HVP (LO) DISC}} = \sum_{t=0}^{\infty} w_t C(t) \quad (9)$$

with appropriately defined w_t . Due to our choice of relatively short time direction with 48 points, special care needs to be taken to control potentially missing long-time contributions in $C(t)$. In the following we estimate these effects quantitatively. Consider the vector operator

$$V_\mu^{f,f'}(x) = \bar{\Psi}_f(x) \gamma_\mu \Psi_{f'}(x) \quad (10)$$

with f and f' denoting quark flavors. Then the Wick contractions

$$\langle V_\mu^{u,u} V_\nu^{u,u} \rangle - \langle V_\mu^{u,d} V_\nu^{d,u} \rangle \quad (11)$$

isolate the light-quark disconnected contribution in the isospin symmetric limit, see also Ref. [31]. Unfortunately there is no similar linear combination (without partial quenching) that allows for the isolation of the strange-quark disconnected contribution. Nevertheless, using

$$\langle (V_\mu^{u,u} - V_\mu^{s,s})(V_\nu^{u,u} - V_\nu^{s,s}) \rangle - \langle V_\mu^{u,d} V_\nu^{d,u} \rangle \quad (12)$$

one can isolate the sum of $C(t) + C_s(t)$, again making use of the isospin symmetry. Since this sum corresponds to a complete set of Feynman diagrams resulting from the

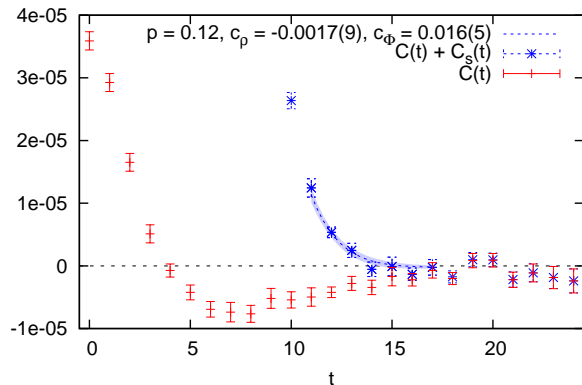


FIG. 3. Zero-momentum projected correlator $C(t)$ and $C(t) + C_s(t)$. A correlated fit of $\rho(770)$ and $\phi(1020)$ exponentials via $c_\rho e^{-E_\rho t} + c_\phi e^{-E_\phi t}$ in the region $t \in [11, \dots, 17]$ to $C(t) + C_s(t)$ yields a p -value of 0.12. We use fixed energies $E_\rho = 770$ MeV and $E_\phi = 1020$ MeV and fit parameters c_ρ and c_ϕ .

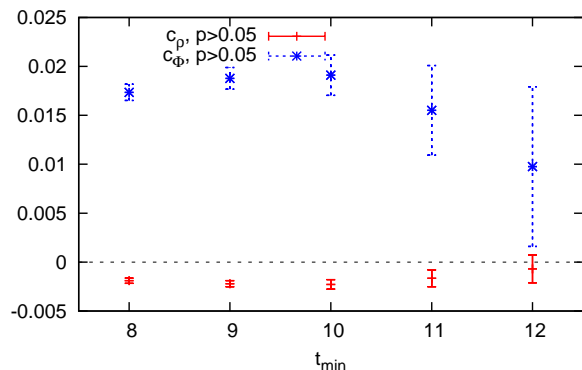


FIG. 4. Coefficients and p -values of a fit of $c_\rho e^{-E_\rho t} + c_\phi e^{-E_\phi t}$ to $C(t) + C_s(t)$ in the region $t \in [t_{\min}, \dots, 17]$.

above Wick contractions, we can represent it as a sum over individual exponentials $C(t) + C_s(t) = \sum_m c_m e^{-E_m t}$ with $c_m \in \mathbb{R}$ and $E_m \in \mathbb{R}^+$. The coefficients c_m can be negative because positivity arguments only apply to some individual Wick contractions in Eq. (12) but not necessarily to the sum.

We show $C(t)$ and $C_s(t)$ obtained in our lattice QCD computation in Fig. 3. Starting from time-slices 17, 18 the correlator $C(t)$ is not well resolved from zero, however, from time-slices 11 to 17 a two-state fit including the $\rho(770)$ and $\phi(1020)$ describes $C(t) + C_s(t)$ well. Here the ρ is a proxy for combined ρ and ω contributions due to their similar energy. Since these states are not stable in our lattice simulation, however, this representation using individual exponentials only serves as a model that fits the data well. Since this model will only enter our systematic error estimate, we find this imperfection to be acceptable. A systematic study of different fit ranges is presented in Fig. 4, where p -values greater than 0.05 are found for all fit-ranges $t \in [t_{\min}, \dots, 17]$ with $t_{\min} \in [8, \dots, 12]$.

We now define the partial sums

$$L_T = \sum_{t=0}^T w_t C(t), \quad (13)$$

$$F_T(r) = \sum_{t=T+1}^{t_{\max}} w_t (c_\rho^r e^{-E_\rho t} + c_\phi^r e^{-E_\phi t} - C_s(t)), \quad (14)$$

where c_ρ^r and c_ϕ^r are the parameters of the fit with fit-range r and $t_{\max} = 24$ for our setup. For sufficiently large T , L_T is expected to exhibit a plateau region as function of T from which we can determine $a_\mu^{\text{HVP (LO) DISC}}$. The sum $L_T + F_T$ is also expected to exhibit such a plateau to the extent that the model in F_T describes the data well.

Based on Fig. 4, we choose $r = [11, \dots, 17]$ as preferred fit-range to determine F_T but a cross-check with $r = [12, \dots, 17]$ has been performed yielding a consistent result. Figure 5 shows the resulting plateau-region for L_T and $L_T + F_T$. In order to avoid contamination of our first-principles computation with the model-dependence of F_T , we determine $a_\mu^{\text{HVP (LO) DISC}}$ from $L_{T=20}$ and include $F_{T=20}$ as systematic uncertainty estimating a potentially missing long-time tail. We choose the value at $T = 20$ since it appears to be safely within a plateau region but sufficiently far from $T = 24$ to suppress backwards-propagating effects [32]. We find $a_\mu^{\text{HVP (LO) DISC}} = -9.6(3.3) \times 10^{-10}$.

We expect the finite lattice spacing and finite simulation volume as well as long-time contributions to Eq. (9) to dominate the systematic uncertainties of our result. With respect to the finite lattice spacing a reasonable proxy for the current computation may be our HVP connected strange-quark analysis [33] for which the 48^3 result at $a^{-1} = 1.73$ GeV agrees within $\mathcal{O}(5\%)$ with the continuum-extrapolated value. This is also consistent with a naïve $\mathcal{O}(a^2 \Lambda_{\text{QCD}}^2)$ power counting, appropriate for the domain-wall fermion action used here. The combined effect of the finite spatial volume and potentially missing two-pion tail is estimated using a one-loop finite-volume lattice-regulated chiral perturbation theory (ChPT) version of Eq. (5.1) of Ref. [31]. Our ChPT computation also agrees with Eq. (2.12) of Ref. [34] after correcting for a missing factor of two in the first version of Ref. [34]. The ChPT result is then transformed to position space to obtain $C(t)$. Fig. 6 shows a corresponding study of L_T for different volumes. We take the difference of $L_{T=20}$ on the $48^3 \times 96$ lattice used here and $L_{T=48}$ on the $96^3 \times 192$ lattice and obtain $\delta a_\mu^{\text{FV}, \pi\pi} = 1.4 \times 10^{-10}$. The remaining long-time effects are estimated by $F_{T=20}$. We compare the result for two fit-ranges $F_{T=20}([11, \dots, 17]) = -1.1(6) \times 10^{-10}$ and $F_{T=20}([12, \dots, 17]) = -0.6(0.9) \times 10^{-10}$. We conservatively take the one-sigma bound $\delta a^{\text{FV}} = 1.7 \times 10^{-10}$ as additional uncertainty.

Combining the systematic uncertainties in quadrature,

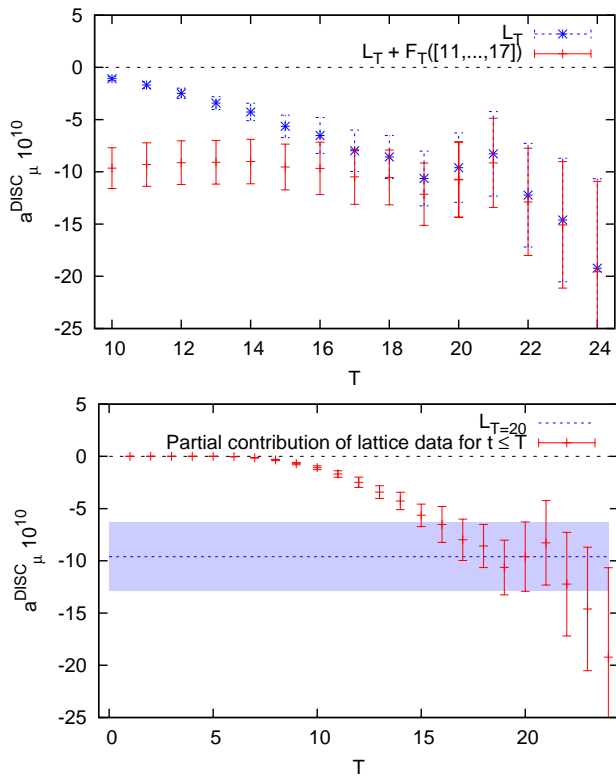


FIG. 5. The sum of L_T and F_T defined in Eqs. (13) and (14) has a plateau from which we read off $a_\mu^{\text{HVP (LO) DISC}}$. The lower panel compares the partial sums L_T for all values of T with our final result for $a_\mu^{\text{HVP (LO) DISC}}$ with its statistical error band.

we report our final result

$$a_\mu^{\text{HVP (LO) DISC}} = -9.6(3.3)(2.3) \times 10^{-10}, \quad (15)$$

where the first error is statistical and the second systematic.

Before concluding, we note that our result appears to be dominated by very low energy scales. This is not surprising since the signal is expressed explicitly as difference of light-quark and strange-quark Dirac propagators. We therefore expect energy scales significantly above the strange mass to be suppressed. We already observed this above in the dominance of low modes of the Dirac operator for our signal. Furthermore, our result is statistically consistent with the one-loop ChPT two-pion contribution of Fig. 6.

CONCLUSION

We have presented the first ab-initio calculation of the hadronic vacuum polarization disconnected contribution to the muon anomalous magnetic moment at physical pion mass. We were able to obtain our result with modest

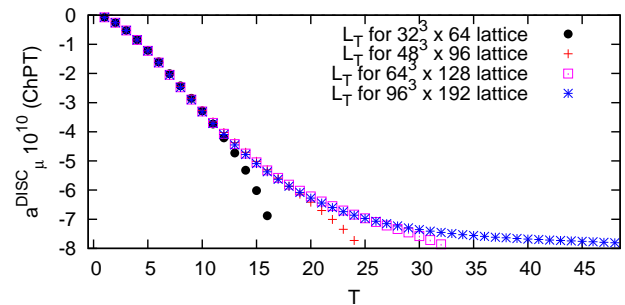


FIG. 6. The leading-order pion-loop contribution in finite-volume ChPT as function of volume.

computational effort utilizing a refined noise-reduction technique explained above. This computation addresses one of the major challenges for a first-principles lattice QCD computation of a_μ^{HVP} at percent or sub-percent precision, necessary to match the anticipated reduction in experimental uncertainty. The uncertainty of the result presented here is already slightly below the current experimental precision and can be reduced further by a straightforward numerical effort.

ACKNOWLEDGMENTS

We would like to thank our RBC and UKQCD collaborators for helpful discussions and support. C.L. is in particular indebted to Norman Christ, Masashi Hayakawa, and Chulwoo Jung for helpful comments regarding this manuscript. This calculation was carried out at the Fermilab cluster pi0 as part of the USQCD Collaboration. The eigenvectors were generated under the ALCC Program of the US DOE on the IBM Blue Gene/Q (BG/Q) Mira machine at the Argonne Leadership Class Facility, a DOE Office of Science Facility supported under Contract De-AC02-06CH11357. T.B. is supported by US DOE grant DE-FG02-92ER40716. P.A.B. and A.P. are supported in part by UK STFC Grants No. ST/M006530/1, ST/L000458/1, ST/K005790/1, and ST/K005804/1 and A.P. additionally by ST/L000296/1. T.I. and C.L. are supported in part by US DOE Contract #AC-02-98CH10886(BNL). T.I. is supported in part by the Japanese Ministry of Education Grant-in-Aid, No. 26400261. L.J. is supported in part by US DOE grant #de-sc0011941. A.J. is supported by EU FP7/2007-2013 ERC grant 279757. K.M. is supported by the National Sciences and Engineering Research Council of Canada. M.S. is supported by EPSRC Doctoral Training Centre Grant EP/G03690X/1.

* Corresponding author; clehner@quark.phy.bnl.gov

- [1] D. Hanneke, S. Fogwell, and G. Gabrielse, *Phys.Rev.Lett.* **100**, 120801 (2008), arXiv:0801.1134 [physics.atom-ph].
- [2] T. Aoyama, M. Hayakawa, T. Kinoshita, and M. Nio, *Phys. Rev.* **D91**, 033006 (2015), arXiv:1412.8284 [hep-ph].
- [3] M. Davier, A. Hoecker, B. Malaescu, and Z. Zhang, *Eur. Phys. J.* **C71**, 1515 (2011), [Erratum: *Eur. Phys. J.* **C72**, 1874(2012)], arXiv:1010.4180 [hep-ph].
- [4] K. Hagiwara, R. Liao, A. D. Martin, D. Nomura, and T. Teubner, *J.Phys.* **G38**, 085003 (2011), arXiv:1105.3149 [hep-ph].
- [5] G. Bennett *et al.* (Muon G-2), *Phys.Rev.* **D73**, 072003 (2006), arXiv:hep-ex/0602035 [hep-ex].
- [6] J. Beringer *et al.* (Particle Data Group), *Phys. Rev.* **D86**, 010001 (2012), including the 2013 update for the 2014 edition at <http://pdg.lbl.gov>.
- [7] R. Carey, K. Lynch, J. Miller, B. Roberts, W. Morse, *et al.*, “The New (g-2) Experiment: A proposal to measure the muon anomalous magnetic moment to ± 0.14 ppm precision,” (2009).
- [8] M. Aoki *et al.*, KEK-J-PARC **PAC2009**, 12 (2009).
- [9] J. Grange *et al.* (Muon g-2), (2015), arXiv:1501.06858 [physics.ins-det].
- [10] A. Kurz, T. Liu, P. Marquard, and M. Steinhauser, *Phys. Lett.* **B734**, 144 (2014), arXiv:1403.6400 [hep-ph].
- [11] J. Prades, E. de Rafael, and A. Vainshtein, *Adv. Ser. Direct. High Energy Phys.* **20**, 303 (2009), arXiv:0901.0306 [hep-ph].
- [12] T. Blum, N. Christ, M. Hayakawa, T. Izubuchi, L. Jin, and C. Lehner, (2015), arXiv:1510.07100 [hep-lat].
- [13] J. Green, O. Gryniuk, G. von Hippel, H. B. Meyer, and V. Pascalutsa, *Phys. Rev. Lett.* **115**, 222003 (2015), arXiv:1507.01577 [hep-lat].
- [14] T. Blum, S. Chowdhury, M. Hayakawa, and T. Izubuchi, (2014), arXiv:1407.2923 [hep-lat].
- [15] V. Gulpers, A. Francis, B. Jager, H. Meyer, G. von Hippel, and H. Wittig, *Proceedings, 32nd International Symposium on Lattice Field Theory (Lattice 2014)*, PoS **LATTICE2014**, 128 (2014), arXiv:1411.7592 [hep-lat].
- [16] G. Bali and G. Endrodi, *Phys. Rev.* **D92**, 054506 (2015), arXiv:1506.08638 [hep-lat].
- [17] F. Burger, G. Hotzel, K. Jansen, and M. Petschlies, (2015), arXiv:1501.05110 [hep-lat].
- [18] B. Chakraborty, C. T. H. Davies, J. Koponen, G. P. Lepage, M. J. Peardon, and S. M. Ryan, (2015), arXiv:1512.03270 [hep-lat].
- [19] B. Toth, “Disconnected contribution to hadron correlation functions,” (2015), the 33rd International Symposium on Lattice Field Theory.
- [20] T. Blum, *Phys.Rev.Lett.* **91**, 052001 (2003), arXiv:hep-lat/0212018 [hep-lat].
- [21] D. Bernecker and H. B. Meyer, *Eur. Phys. J.* **A47**, 148 (2011), arXiv:1107.4388 [hep-lat].
- [22] X. Feng, S. Hashimoto, G. Hotzel, K. Jansen, M. Petschlies, *et al.*, *Phys.Rev.* **D88**, 034505 (2013), arXiv:1305.5878 [hep-lat].
- [23] The appropriate normalization factors of Z_V^2 are of course included in our computation.
- [24] J. Foley, K. Jimmy Juge, A. O’Cais, M. Peardon, S. M. Ryan, and J.-I. Skullerud, *Comput. Phys. Commun.* **172**, 145 (2005), arXiv:hep-lat/0505023 [hep-lat].
- [25] A. Li *et al.* (xQCD), *Phys. Rev.* **D82**, 114501 (2010), arXiv:1005.5424 [hep-lat].
- [26] R. C. Brower, H. Neff, and K. Orginos, *Lattice field theory. Proceedings, 22nd International Symposium, Lattice 2004, Batavia, USA, June 21-26, 2004*, *Nucl. Phys. Proc. Suppl.* **140**, 686 (2005), [686(2004)], arXiv:hep-lat/0409118 [hep-lat].
- [27] T. Blum *et al.* (RBC, UKQCD), (2014), arXiv:1411.7017 [hep-lat].
- [28] T. Blum, T. Izubuchi, and E. Shintani, (2012), arXiv:1208.4349 [hep-lat].
- [29] E. Shintani, R. Arthur, T. Blum, T. Izubuchi, C. Jung, and C. Lehner, (2014), arXiv:1402.0244 [hep-lat].
- [30] C. Jung, “zMobius and other recent developments on Domain Wall Fermions,” (2015), the 33rd International Symposium on Lattice Field Theory.
- [31] M. Della Morte and A. Jüttner, *JHEP* **11**, 154 (2010), arXiv:1009.3783 [hep-lat].
- [32] Alternatively taking $T = 21$ instead of $T = 20$ and repeating our procedure to estimate systematic uncertainties, we find $a_\mu^{\text{HVP (LO) DISC}} = -8.3(4.0)(1.8) \times 10^{-10}$, where the first error is statistical and the second systematic. This value is consistent with our preferred value, however, has a different balance of statistical and systematic errors.
- [33] M. Spraggs, “The strange contribution to $a_\mu^{\text{HVP,LO}}$ with physical quark masses using Mobius domain wall fermions,” (2015), the 33rd International Symposium on Lattice Field Theory.
- [34] C. Aubin, T. Blum, P. Chau, M. Golterman, S. Peris, and C. Tu, (2015), arXiv:1512.07555 [hep-lat].

In the following we add additional plots supplementing relevant technical details regarding our results. Figs. 7–11 are for physical pion mass. Figs. 12 and 13 are for heavy pion mass $m_\pi = 422$ MeV. The results for heavy pion mass are obtained from only 6 configurations of the RBC and UKQCD $24^3 \times 64$ lattice. The AMA setup uses 45 sloppy solves and 4 exact solves per configuration [28, 29].

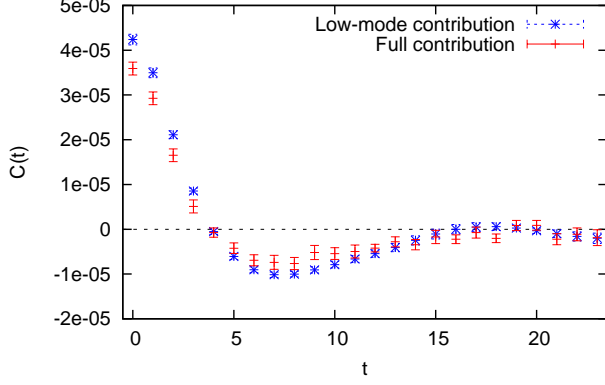


FIG. 7. The low-mode contribution to $C(t)$ is contrasted with the full result. As mentioned in the main text, the signal is mostly saturated by the low modes.

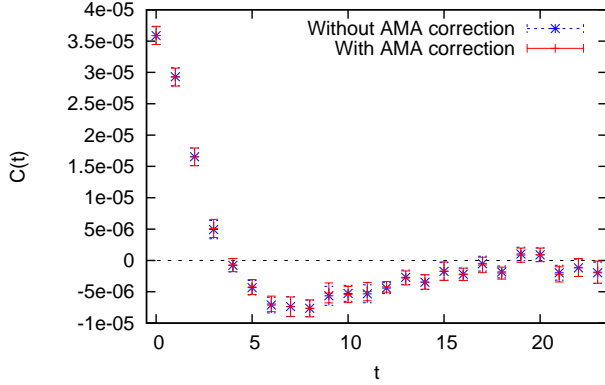


FIG. 8. The correlator $C(t)$ is plotted with and without the AMA correction term. The noise of the AMA estimator is dominated by the sloppy solves.

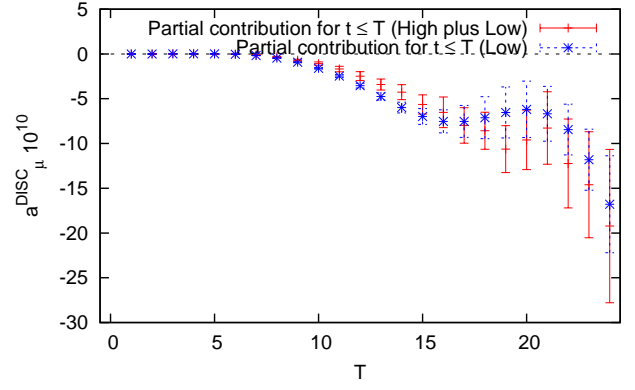


FIG. 9. The partial sum L_T is plotted with and without the high-mode contribution. The similar uncertainty at around $T \approx 20$ suggests that the additional high-mode noise is well controlled and that the noise is dominated by gauge-field fluctuations.

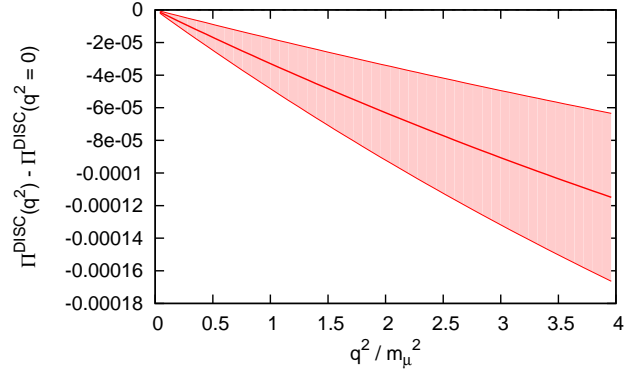


FIG. 10. The subtracted scalar vacuum polarization function $\Pi^{\text{DISC}}(q^2)$ for the disconnected contribution from our physical-pion-mass lattice data is plotted in the interesting region of $q^2 \in [0, 4m_\mu^2]$. The shaded band corresponds to the statistical uncertainty of our result.

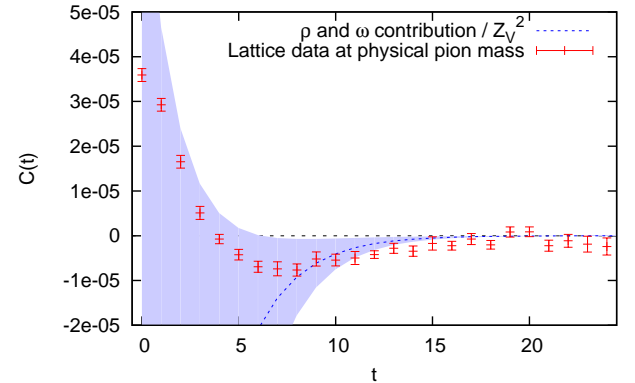


FIG. 11. The long-distance model based on ρ and ω resonances used quantitatively in Ref. [18] is shown on top of our lattice data at physical pion mass. The shaded region corresponds to the parametric uncertainty of the model prediction with central value shown as dashed line.

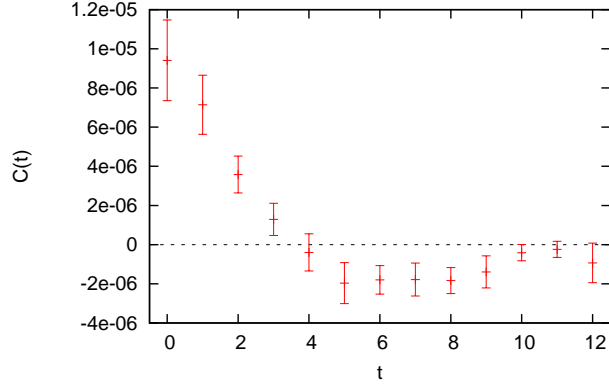


FIG. 12. The correlator for heavy pion mass $m_\pi = 422$ MeV.

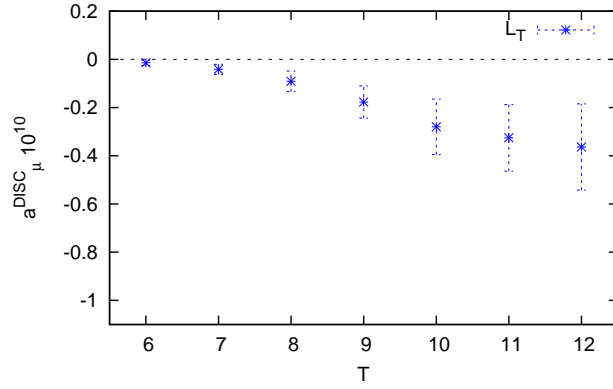


FIG. 13. For heavy pion mass $m_\pi = 422$ MeV, we find a very small result for the HVP disconnected contribution, $a_\mu \approx -0.4(2) \times 10^{-10}$, consistent with the results of Ref. [18] at similar pion mass.